

Learnable Graph Inception Network for Emotion Recognition

Amir Shirian
University of Warwick

Subarna Tripathi
Intel Labs

Tanaya Guha
University of Warwick

ABSTRACT

Analyzing emotion from verbal and non-verbal behavioral cues is critical for many intelligent human-centric systems. The emotional cues can be captured using audio, video, motion-capture (mocap) or other modalities. We propose a generalized graph approach to emotion recognition that can take any time-varying (dynamic) data modality as input. To alleviate the problem of optimal graph construction, we cast this as a joint graph learning and classification task. To this end, we present the *Learnable Graph Inception Network* (L-GrIN) that jointly learns to recognize emotion and to identify the underlying graph structure in data. Our architecture comprises multiple novel components: a new graph convolution operation, a graph inception layer, learnable adjacency, and a learnable pooling function that yields a graph-level embedding. We evaluate the proposed architecture on four benchmark emotion recognition databases spanning three different modalities (video, audio, mocap), where each database captures one of the following emotional cues: facial expressions, speech and body gestures. We achieve state-of-the-art performance on all databases outperforming several competitive baselines and relevant existing methods.

KEYWORDS

emotion recognition, graph neural network, graph learning, emotion in multimedia

1 INTRODUCTION

Automated analysis and recognition of human emotion from verbal (speech) and non-verbal behavioral cues (e.g. facial expressions, body gestures) is critical for human-centric systems involving human-machine interaction, with applications ranging from driver's safety [1] to behavioral healthcare [2] to human-robot conversational systems [3]. The behavioral cues can be captured using audio, video, motion capture (mocap) or other sensors. In general, emotion recognition in any modality is a challenging task due to the huge variability and subjectivity involved in the expression and perception of emotion. In recent years, significant progress has been made towards the recognition and analysis of emotion using dynamic facial expressions [4–8], speech [9–12] and body gestures [13–15]. Since human emotion is inherently multimodal, research efforts that combine information from multiple modalities are also on the rise [16, 17].

In the literature of dynamic emotion recognition, architectures based on recurrent neural networks (RNN) are common [12, 18, 19]. Such networks often have complex architecture with millions of trainable parameters [20], and are trained with large amount of data. A compact, efficient and scalable way to represent data is in the form of graphs. Motivated by the recent success of graph convolutional network (GCN) in action recognition [21], we propose to adopt a graph approach to represent emotion dynamics. Subsequently, we cast emotion recognition as a joint graph learning and

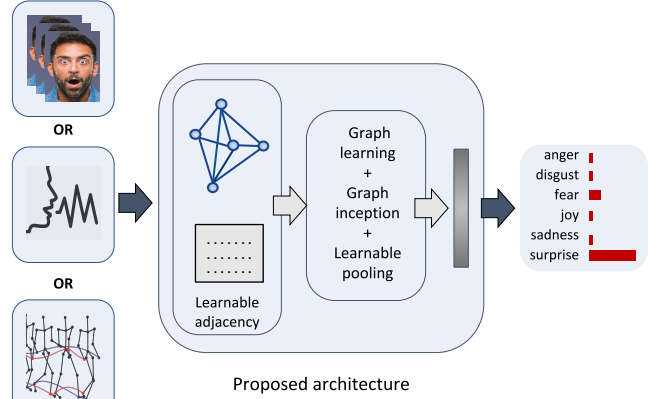


Figure 1: A generalized graph approach to emotion recognition from dynamic input data. Data samples are transformed to a *learnable* graph structure, where each node corresponds to a short temporal segment or frame. A novel graph inception network (L-GRIN) produces an embedding for the entire graph facilitating emotion recognition.

graph classification problem. In our approach, each dynamic data sample is represented as a graph, where each node corresponds to a short temporal segment in the data. Each node contains the features extracted from a short temporal segment (frame) as its node attribute. Note that our architecture is not tied to landmark point locations as node attributes, and can be replaced by any other relevant information or even, embeddings from a pretrained network.

Note that the graph structure i.e., the edge weights connecting the nodes is not naturally defined here. When a graph structure is not known apriori, a common practice is to manually construct the graph. This, however, results into sub-optimal graphs. We thus propose to learn the graph structure itself during the training stage. This is a generalized formulation, where the temporal dependencies between the nodes are automatically discovered. The only assumption we make is that the graph structure remains the same for all videos for this task. To this end, we propose a novel GCN architecture, the *learnable graph inception network* (L-GrIN), with several novel components: a newly defined graph convolution that uses a non-linear layer-wise projection technique, introduction of an inception module in graph domain, learnable graph structure and learnable graph-to-vector pooling function. Our architecture produces superior results on four benchmark emotion recognition databases spanning three different modalities (video, audio, mocap). Each database captures one of the following emotional cues: facial expressions, speech and body gestures. In summary, the main contributions of this paper are:

- A generalized graph approach that combines graph learning and graph classification to address the problem of emotion recognition for dynamic input.
- A novel graph architecture, **L-GrIN**, with a new convolution layer, an graph inception module, learnable graph structure and learnable pooling.
- State-of-the-art performance for facial, speech and body emotion recognition on four benchmark databases spanning three disparate modalities.

2 RELATED WORK

In this section, we review the related work in the areas of GCNs and emotion recognition using various modalities.

Graph neural network. Deep learning on graph data has emerged as a major topic in the past few years. This is because graphs provide a natural and convenient way to deal with large data. Among the different graph neural networks, GCNs have received the most attention [22–24]. GCNs have wide applications in computer vision, natural language processing, social network analysis, and even in problems arising in physics, chemistry and biology [25, 26]. GCNs have been successfully applied in various image and video-based applications, such as face clustering [27], object detection [28], visual reasoning [29], and in image generation using scene graphs [30, 31]. GCNs have been used to address skeleton-based action recognition [21, 32] recorded using a mocap system. In speech, the application of graph networks have started emerging in automatic speech recognition [33].

The GCNs can be broadly classified into two categories: *spatial* and *spectral*. The spatial GCNs imitate the convolution operation of the CNNs by aggregating the information from neighboring nodes [22, 34, 35]. The problem of different graph nodes having different number of neighbours is usually addressed by using a fixed size neighborhood [35] or by converting graph structures into a regular grid and subsequently applying traditional CNNs [36]. A recent work proposed to develop the graph structure considering the Weisfeiler-Lehman graph isomorphism test [37], and achieved state-of-the-art performance in node classification task in citation networks. On the other hand, the spectral GCNs formulate the convolution operation as a frequency domain filtering operation following the theory of signal processing [38], where convolution filters are seen as a set of learnable parameters. Later the ChebNet [39] was proposed to reduce the computational cost of spectral GCNs, which redefined the convolution filter in terms of Chebyshev polynomials bypassing the need to eigen decomposition of the graph Laplacian. In a follow-up work [23], a first order approximation of the Chebyshev polynomials was introduced. This further simplified the spectral GCN computation as the convolution operation reduces to a linear projection.

Emotion recognition. Here we briefly review the recent works on facial, speech and body emotion recognition. To the best of our knowledge, graph-based networks have not been employed for any of these tasks.

Facial emotion recognition. Recognizing facial expressions is the most common way of analyzing emotion. The majority of work rely on identifying an individual’s facial expression from images or

videos (fewer work on videos), and associating them to one of the basic emotion classes. Recent efforts in image-based recognition are focused on using CNNs and its variants [4, 40], and also on using adversarial learning [41]. Few works have proposed to use attention networks to account for the context [6, 42, 43]. RNNs and 3D CNNs have been used for video-based emotion recognition due to their ability to capture the temporal information [20, 44]. Another line of work focuses on the dynamics of landmark points in faces extracted from videos. In this context, a deep temporal appearance geometry network has been proposed [45] that uses the landmark point geometry and a CNN for emotion recognition. Another recent work constructed a trajectory matrix from the landmark points and used them as inputs to a CNN [46].

Speech emotion recognition. Speech emotion recognition has been studied widely in the past years. Many speech emotion recognition systems rely on acoustic, prosodic and lexical features [47, 48] which are then fed to deep networks for classification [19, 49–51]. Recently many deep architectures have been proposed for this task, among which RNN-based architecture are most common [18, 51–53] due to their ability to capture the temporal information. Attention techniques also have been shown to be successful in recognizing emotion in speech [18, 53]. Representation learning has also been investigated [54] for this task. An end-to-end recognition system combining CNN and long short term memory (LSTM) network has also been proposed [52].

Body emotion recognition. Body expressions are relatively less studied in emotion recognition. The existing body of work is focused on using motion information in terms of low-level descriptors such as joint angles, 3D positions, distance between joints, velocity and acceleration [55–57]. A trajectory learning approach [55] proposes to identify ‘neutral’ motion from input data, and used the deviation of a given input from the neutral motion as a feature for classifying emotions. Another recent work combined deep features with psychological attributes to detect emotion from 3D body pose using a random Forest classifier [56]. Gait information has also been considered for recognizing emotion, where a spatial GCN is used to detect the emotional state [57].

3 PROPOSED APPROACH

In this section, we describe our deep graph approach to emotion recognition. First, we construct a graph from dynamic input data following a generalized frame-to-node approach. Next, we propose a novel architecture, called L-GrIN, that jointly performs graph learning and graph classification. This is achieved by optimizing over a new loss function that combines classification loss and a graph structure loss. L-GrIN defines a new graph convolution layer, introduces an inception module in graph domain, learns the adjacency matrix (graph learning) and also a pooling function to learn a graph-level representation from its node embeddings. The proposed architecture, L-GRIN, is illustrated in Fig. 2. Below, we describe each component in detail.

3.1 Graph construction

Given a time-varying input sequence, our first task is to construct an undirected graph $\mathcal{G} = (\mathcal{V}, \mathcal{E})$ that can efficiently capture the emotion-related dynamics in the data, where \mathcal{V} is the set of nodes

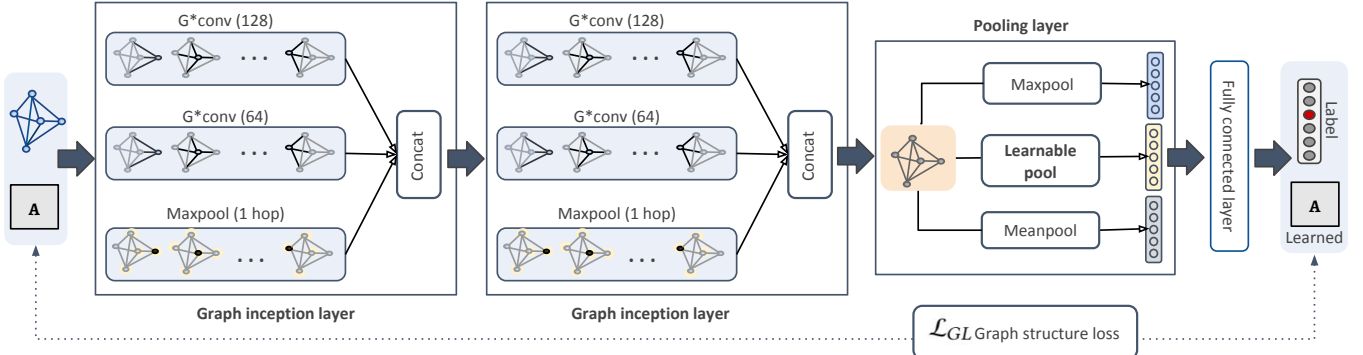


Figure 2: Our proposed architecture, L-GRIN, consists of two graph inception layers (with a new spectral graph convolution layer) and a Pooling layer (with two fixed pooling layers and a learnable pooling layer). The Inception layers given graph input produce node level representation which are pooled to obtain a graph-level representation in the Pooling layer. L-GRIN also learns the underlying graph structure (adjacency matrix) by jointly optimizing a classification loss and a graph structure loss.

with cardinality $|\mathcal{V}| = M$ and \mathcal{E} is the set of all edges between the connected nodes. A representative description of \mathcal{G} is typically given by an adjacency matrix $\mathbf{A} \in \mathbb{R}^{M \times M}$ which is symmetric for an undirected graph.

Our graph construction approach follows a *frame-to-node* transformation, where M frames in the data form the M graph nodes $\{v_i\}_{i=1}^M \in \mathcal{V}$ (see Fig. 3). A frame refers to a small temporal segment of the data, for example, an audio segment of length 40ms. In order to encode the temporal information, a frame (node) should be connected with weights to a series of past and future nodes. An element $(\mathbf{A})_{ij} \in \mathbf{A}$ contains the weight corresponding to the edge $e_{ij} \in \mathcal{E}$ connecting v_i and v_j . Note that the graph structure is not naturally defined here, i.e., the elements in \mathbf{A} are unknown. A common way to define the elements in \mathbf{A} is through constructing a distance function manually [21]. This may result into a sub-optimal graph representation. Hence, we propose to learn the elements in \mathbf{A} by jointly optimizing a structural loss combined with a classification loss. This loss function will be discussed in Section 3.2.

In order to capture the emotion content at node-level, we rely on modality-specific features or even, raw data. Each node v_i is thus associated with a *node feature* vector $\mathbf{n}_i \in \mathbb{R}^P$. A feature matrix $\mathbf{N} \in \mathbb{R}^{M \times P}$ consisting all the node feature vectors is defined as $\mathbf{N} = [\mathbf{n}_1, \mathbf{n}_2, \dots, \mathbf{n}_M]^T$. Feature extraction for individual modalities is discussed in Section 4.

3.2 Learnable graph inception network

Given a set of (dynamic inputs transformed to) graphs $\{G_1, \dots, G_N\}$ and their true labels $\{y_1, \dots, y_N\}$ represented as one-hot vectors, our task is to develop a GCN architecture that is able to recognize the emotional content in the data. Since the graph structure is not naturally defined here, we propose to learn an optimal \mathbf{A} from the training data with the underlying assumption that each graph has different node features but the same edge weights. We formulate this as a joint graph learning and graph classification problem.

Background. A common GCN architecture takes the node feature matrix $\mathbf{N} \in \mathbb{R}^{M \times P}$ and the graph adjacency matrix \mathbf{A} as inputs and produces a *node-level* representation matrix $\mathbf{Z} \in \mathbb{R}^{M \times Q}$, where

Q is the dimension of the output feature vector at each node. A GCN layer $\mathbf{H}^{(k+1)}$ can be defined as a non-linear function of its previous layer as follows

$$\mathbf{H}^{(k+1)} = \sigma(\mathbf{A}\mathbf{H}^{(k)}\mathbf{W}^{(k)}) \quad (1)$$

where $\mathbf{W}^{(k)}$ is the weight matrix for the k^{th} layer of the neural network, σ is a non-linear activation function, such as a ReLU, and k is the layer number ($k = 0, \dots, K$). Note that $\mathbf{H}^{(0)} = \mathbf{N}$ and $\mathbf{H}^{(K)} = \mathbf{Z}$. An effective improvement on this propagation rule has been recently proposed [23].

$$\mathbf{H}^{(k+1)} = \sigma(\mathbf{D}^{-\frac{1}{2}}(\mathbf{A} + \mathbf{I})\mathbf{D}^{-\frac{1}{2}}\mathbf{H}^{(k)}\mathbf{W}^{(k)}) \quad (2)$$

where \mathbf{D} is the degree matrix of \mathbf{A} , and \mathbf{I} is an $M \times M$ identity matrix. Note that the terms within the parenthesis in Eq. (2) is simply a linear projection, and can be re-written as

$$\mathbf{H}^{(k+1)} = \sigma(\hat{\mathbf{A}}\mathbf{H}^{(k)}\mathbf{W}^{(k)}) \quad (3)$$

where $\hat{\mathbf{A}} = \mathbf{D}^{-\frac{1}{2}}(\mathbf{A} + \mathbf{I})\mathbf{D}^{-\frac{1}{2}}$.

Proposed network. We present a new GCN architecture, called L-GRIN (see Fig. 2), for joint graph learning and classification. It has the following four new components:

- **Non-linear spectral graph convolution ($\mathcal{G}^*\text{conv}$).** Motivated by a recent work on spatial graph neural network [24], we replace the linear projection in (3) by a multi-layer perceptron (MLP) layer, and replace $\hat{\mathbf{A}}$ by a learnable \mathbf{A} . Thus, instead of the linear layer in (3), we define a new spectral graph convolution layer $\mathcal{G}^*(\cdot)$ as follows:

$$\mathcal{G}^*(\mathbf{H}^{(k)}) = \sigma\left(\text{MLP}^{(k)}(\text{ReLU}(\mathbf{A})\mathbf{H}^{(k)})\right) \quad (4)$$

where $\text{MLP}(\cdot)$ has two hidden layers with η neurons each, \mathbf{A} is the learnable adjacency matrix and σ is a nonlinear activation function. \mathbf{A} is learned through a joint optimization process described later in this section. The $\text{ReLU}(\cdot)$ in Eq. (4) ensures the non-negativity of \mathbf{A} . We refer to the convolution operation defined above as $\mathcal{G}^*\text{conv}$ in the rest of the paper.

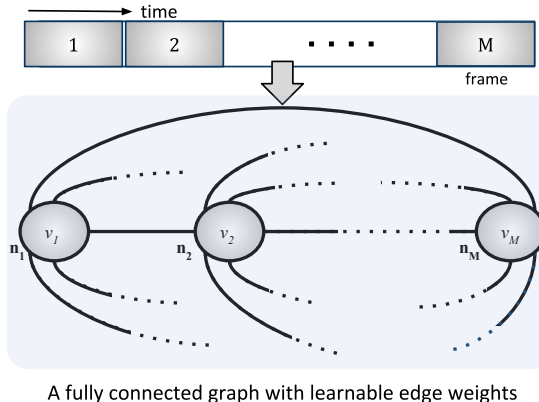


Figure 3: Graph construction: Given a dynamic input sequence of M segments, a fully-connected graph with M nodes is constructed. Each node corresponds to a temporal segment (frame), and is associated with a node attribute vector. The edge weights are learned during the training phase.

- **Graph inception.** We extend the idea of inception layer in traditional CNNs [58] to the graph domain, and introduce a *graph inception* module in our architecture (see Fig. 2). Our graph inception layer consists of two graph convolution layers and one maxpool layer operating on directly connected (1-hop) neighbours only.

Given an input $\mathbf{H}^{(k)}$, the proposed graph inception layer is defined as follows:

$$\mathbf{H}^{(k+1)} = [\mathcal{G}_1^*(\mathbf{H}^{(k)}) \mid \mathcal{G}_2^*(\mathbf{H}^{(k)}) \mid \text{maxpool}(\mathbf{H}^{(k)})] \quad (5)$$

where \mid denotes concatenation of the node features, and \mathcal{G}_1^* and \mathcal{G}_2^* are two \mathcal{G}^* conv layers (see Eq. (4)) with different size of their MLP layers ($\eta = 128$ for \mathcal{G}_1^* and $\eta = 64$ for \mathcal{G}_2^*). Hence, for an input of $\mathbf{H}^{(k)} \in \mathbb{R}^{M \times P}$, the inception layer produces an output $\mathbf{H}^{(k+1)} \in \mathbb{R}^{M \times (128+64+P)}$.

The two \mathcal{G}^* conv layers that yield embeddings of different dimensions can be interpreted as a *multiscale analysis* on graphs in spectral domain. Like a traditional inception layer in CNN, our graph inception layer also combines features from multiple scales allowing the network to have both width and depth. Our graph inception layer has fewer parameters (compared to inception networks in CNNs) enabling us to feed the input directly to the inception layer.

The maxpool function in Eq. (5) operates on every node separately. For each node v_i , we only consider its directly connected neighbors (1-hop), and maxpool over the embeddings along feature dimension. Note that, since we start with a fully-connected graph, initially this operation is the same as maxpooling over all nodes, but this changes quickly as we start discovering the graph structure.

- **Learnable pooling for graph-level representation.** Our objective is to classify entire graphs, as opposed to the more common task of classifying each node. Hence, we seek a *graph-level* representation $\mathbf{h}_G \in \mathbb{R}^Q$ as the output of our network. This can be

obtained by pooling the node-level representations $\mathbf{H}^{(k)}$ at the K -th layer before passing them to the classification layer (see Fig. 2). Common choices for pooling functions in graph domain are mean, max and sum pooling [23, 35]. Max and mean pooling often fail to preserve the underlying information about the graph structure while sum pooling is shown to be a better alternative [24]. However, all these pooling functions treat every neighboring node with equal importance, which may not be optimal. To this end, we propose to *learn* a pooling function Ψ that combines the node embeddings from the K -th layer to produce an embedding for the entire graph. Additionally, we also use maxpool and meanpool and combine all the graph-level embeddings together. The pooling layer is thus defined as follows:

$$\mathbf{h}_G = [\text{maxpool}(\mathbf{H}^{(K)}) \mid \Psi(\mathbf{H}^{(K)}) \mid \text{meanpool}(\mathbf{H}^{(K)})] \quad (6)$$

$$\Psi(\mathbf{H}^{(K)}) = \mathbf{H}^{(K)} \mathbf{p}$$

where \mathbf{p} has learnable weights to combine node-level embeddings to obtain a graph-level embedding.

- **Learnable adjacency (A).** Recall that in our task the graph structure is not known. Although we can define such structure manually, results are sub-optimal. An effective approach would be to learn the graph structure (adjacency matrix) itself by jointly optimizing over a classification loss and graph learning loss. We assume that all videos have the same underlying graph structure containing the same number of nodes and edges. This largely simplifies our task of graph structure learning. The overall loss \mathcal{L} for joint graph learning and classification is composed of two components: (i) \mathcal{L}_{GC} : a graph classification loss, and (ii) \mathcal{L}_{GL} : a graph learning loss. The classification loss \mathcal{L}_{GC} is defined as the cross-entropy loss:

$$\mathcal{L}_{GC} = - \sum_{n=1}^N \mathbf{y}_n \log \hat{\mathbf{y}}_n \quad (7)$$

where $\hat{\mathbf{y}}_n$ is the predicted label for the n^{th} sample. The graph learning loss, \mathcal{L}_{GL} , is designed to facilitate learning the pooling vector \mathbf{p} and the adjacency matrix \mathbf{A} . This is defined as follows:

$$\mathcal{L}_{GL} = \underbrace{\lambda_1 \mathbf{e}^T (\mathbf{A}_d \odot \mathbf{A}) \mathbf{e} + \lambda_2 \|\mathbf{A}\|_F^2}_{\text{graph structure loss}} + \underbrace{\lambda_3 \|\mathbf{p}\|_2^2}_{\text{learnable pooling}} \quad (8)$$

where \odot denotes element-wise multiplication, \mathbf{e} is an all-ones vector, $\|\cdot\|_F$ denotes Frobenius norm, λ_1 , λ_2 , and λ_3 control the relative weights of the three terms, and \mathbf{A}_d is a structure matrix defined as follows:

$$(\mathbf{A}_d)_{ij} = (i - j)^2 \quad (9)$$

The structure matrix \mathbf{A}_d forces the nodes that are temporally close to each other to have stronger relationship, i.e. higher weights in the \mathbf{A} . The larger the squared distance between two nodes v_i and v_j (frames), the smaller will be the weights in $(\mathbf{A})_{ij}$. The ReLU operation (see Eq. (4)) ensures the non-negativity of the elements in \mathbf{A} . The overall optimization is thus as follows:

$$\min_{\mathbf{A}, \mathbf{p}, \Theta^{(1:k)}} \mathcal{L} = \min_{\mathbf{A}, \mathbf{p}, \Theta^{(1:k)}} [\mathcal{L}_{GC} + \mathcal{L}_{GL}]$$

where, Θ denotes all other learnable network parameters across all graph convolution layers including its constituent MLP layers.



Figure 4: Sample video frames from the RML database showing detected landmark points for four expressions - anger, disgust, fear and joy.

Table 1: Facial emotion recognition: Results and comparisons on the RML and RAVDESS databases.

Model	Accuracy (%)		Parameters
	RML	RAVDESS	
*BLSTM (baseline)	60.00	56.14	~ 1 M
*GCN [23](baseline)	76.57	69.34	~ 102 K
*PATCHY-SAN [35]	80.00	73.52	~ 52 K
*PATCHY-Diff [61]	85.59	79.83	~ 71 K
SENet [40]	71.20	71.06	~ 26 M
AVEF [62]	82.48	-	-
KCFA [63]	82.22	-	-
OKL [64]	90.83	-	-
TJE [65]	-	72.30	-
*L-GrIN	94.11	85.65	~ 120 K

*use same node features

Every term in the overall loss function \mathcal{L} is differentiable, thereby allowing an end-to-end optimization.

4 EXPERIMENTS

In this section, we present extensive experimental results and analysis to evaluate the performance of the proposed architecture for facial, speech and body emotion recognition.

4.1 Facial emotion recognition

Databases. We use two large video emotion recognition databases for our experiments. The databases chosen based on their popularity in emotion recognition literature and their larger size.

The **RML** database [59] contains 720 videos of 6 basic emotions: *anger, disgust, fear, joy, sadness, surprise* collected when the subjects speak. The subjects are from various ethnic groups and speak different languages.

The **RAVDESS** database [60] contains 4904 videos labeled with 8 classes: *anger, calmness, disgust, fear, joy, neutral, sadness and surprise*. This is the largest video emotion database currently available.

Node features. The databases we use provide only raw video clips. Instead of using raw video frames, we choose to use facial

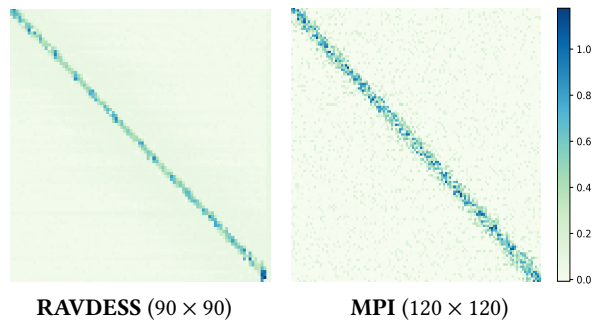


Figure 5: The *learned adjacency matrices* for facial and body emotion recognition. Darker pixels indicate higher values.

landmark points as node attributes. This is because landmark points are known to effectively capture the facial dynamics [66]. We extract 68 landmark points at every video frame using a state-of-the-art landmark detection method [67] (see Fig. 4), resulting into node feature vectors of dimension $P = 136$.

Implementation details. We use a 10-fold cross-validation for both databases, and report the average recognition accuracy in Table 1. We fix the length of each input video to 90 frames yielding a graph with $M = 90$ nodes. The shorter videos are simply padded by duplicating frames from the beginning of the video (cyclic padding). Our network weights are initialized following the Xavier initialization [68]. We set $\lambda_1 = 0.1$ and $\lambda_2 = \lambda_3 = 0.0001$ (see Eq. 8). We used Adam optimizer with a learning rate of 0.01 and decay rate of 0.5 after each 50 epochs for all experiments. To initialize the learnable adjacency matrix \mathbf{A} , we generate a random matrix whose elements are drawn from a Normal distribution with zero mean and unit variance. We used Pytorch for implementing our model and the baselines, and an NVIDIA RTX-2080Ti GPU for all experiments.

Baselines, state-of-the-art. We compare our model against two competitive and relevant baselines as follows:

(i) **BLSTM.** The first baseline is a Bidirectional LSTM (BLSTM), an extension of the traditional LSTMs [69–71]. LSTM and its variants have been successfully used in sentiment analysis in language and speech [18, 72]. This BLSTM comprises 1-layered bidirectional cells with embedding size 300 followed by a fully connected layer.

(ii) **GCN [23].** A natural baseline to compare with our model is a spectral GCN in its standard form (as in Eq. (3)). The original network [23] is designed for node classification and only yields node-level embeddings. To obtain a graph-level embedding, we used max and mean pooling at the end of convolution layers. The GCN uses a binary adjacency matrix constructed following the method used in graph-based action recognition [21].

In addition to the baselines, we compare with two state-of-the-art graph architectures: **PATCHY-SAN** [35] and **PATCHY-Diff** [61]. PATCHY-SAN is recent architecture that learns CNNs for arbitrary graphs for graph classification [35]. PATCHY-Diff is referred to an architecture where PATCHY-SAN is used in combination with a differentiable pooling layer between graph convolution layers [61].

We also compare our model with SENet [40] - a state-of-the-art CNN architecture recently proposed for facial emotion recognition

Table 2: Cross-corpus performance of proposed L-GrIN.

Trained on	Evaluated on	Accuracy (%)
RAVDESS	RML	81.94
RML	RAVDESS	75.42
eINTERFACE	RML	79.86
eINTERFACE	RAVDESS	77.51

in videos. Comparisons are also made with other existing works on the respective databases: audio-visual emotion fusion (AVEF) [62], kernel crossmodal factor analysis (KCFA) [63], optimized kernel-Laplacian (OKL) [64] and temporal joint embeddings (TJE) [65].

Results. Table 1 compares the performance of L-GrIN with all the methods mentioned above. Clearly, the proposed model outperforms all the existing methods by a significant margin, including the graph-based state-of-the-art architectures, such as PATCHY-SAN and PATCHY-Diff. Our model performs better than BLSTM - a class of classifier most commonly used in video-based emotion recognition. SENet is a very recent CNN architecture, which also trails our model in terms of performance. When compared to the GCN baseline [23], L-GrIN improves the recognition accuracy by more than 10% on RML, and more than 5% on RAVDESS. Note that KCFA, OKL and TJE use both audio and visual information for recognition. Our model, even though uses only visual information, shows significant improvement over these audiovisual methods. Fig. 5 shows the learned adjacency matrix for the RAVDESS database. Clearly, the learned graph structure shows higher values closer to the diagonal, i.e. the weights associated among the neighboring nodes. This indicates higher temporal dependencies locally, and weaker dependency as we go further from a node.

Cross-corpus performance. Methods exhibiting superior performance on one corpus, often fall short when tested on another corpus having different statistical distributions. We investigated the ability of our model to generalize across data by evaluating its cross-corpus performance. To this end, we trained *L-GrIN* on one database, followed by fine-tuning a fully-connected layer on the target database, without changing the graph structure (or other parameters) learned from the training database. We also trained on a completely different video-based emotion recognition database (called eINTERFACE [73]) and tested on both RML and RAVDESS.

Results in Table 2 shows that our model can generalize quite well, and produces consistent results under cross-corpus training. The cross-corpus performance shows 6 – 8% higher accuracy on RAVDESS and 3 – 5% higher accuracy on RML as compared to the same-corpus accuracy obtained using the GCN baseline. Cross-corpus results are comparable with the same-corpus performance of PATCHY-SAN. This shows the strength of the proposed architecture. It is worth noticing that the RML database (when used for training) does not have *neutral* and *calmness* emotion classes, but our model still recognizes those emotions on RAVDESS with 67.2% and 73.4% accuracy.

Table 3: Speech emotion recognition: Results and comparisons on IEMOCAP database.

Model	Accuracy (%)	Parameters
*BLSTM (baseline)	58.04	~ 0.8 M
*GCN (baseline)	56.14	~ 78 K
*PATCHY-SAN [35]	60.34	~ 60 K
*PATCHY-Diff [61]	63.23	~ 68 K
CNN [51]	58.52	-
CNN-LSTM [51]	59.23	-
Rep learning [54]	50.40	-
LSTM-CTC [19]	64.20	-
*L-GrIN	65.50	~ 92 K

* use same node features

4.2 Speech emotion recognition

Databases. We use the popular IEMOCAP database [74] for evaluating the performance of our model on speech emotion recognition. This database contains a total of 12 hours of data recorded in 5 sessions, where each session contains utterances from two speakers. The final database contains a total of 5531 utterances: 1103 *angry*, 1708 *neutral*, 1636 *happy* and 1084 *sad*.

Node features. We extract a set of low-level descriptors (LLDs) from the raw speech utterances as proposed for Interspeech2009 emotion challenge [47] using the OpenSMILE toolkit [75]. The feature set includes Mel-frequency cepstral coefficients (MFCCs), zero-crossing rate, voice probability, fundamental frequency (F0) and frame energy. For each sample, we use a sliding window of length 25ms with a stride length of 10ms to extract the LLDs locally. Each feature is then smoothed using a moving average filter, and the smoothed version is used to compute their respective first order delta coefficients. Moreover, motivated by a recent work on speech emotion recognition [76], we also add spontaneity as a binary feature. The spontaneity information comes with the database. Altogether this produces node feature vectors of dimension $P = 35$.

Implementation details. Each audio sample produces a graph of $M = 120$ nodes, where each node corresponds to a (overlapping) speech segment of length 25ms. Cyclic padding is used to make the samples of equal length as before. We perform a 5-fold cross-validation and report the average unweighted accuracy in Table 3. All other parameters and settings remain the same as before.

Baselines, state-of-the-art. Our model is compared with two baselines (BLSTM and GCN), two state-of-the-art graph-based architectures (PATCHY-SAN and PATCHY-Diff) as before. In addition, we also compare our model with four state-of-art methods in speech emotion recognition: CNN [51], CNN-LSTM [51], representation learning [54] and LSTM connectionist temporal modeling (LSTM-CTC) [19].



Figure 6: Motion capture recording set-up for the MPI database showing an actor posing for (left to right) T pose (reference), neutral and pride pose.

Table 4: Body emotion recognition: Results and comparisons on the MPI database.

Model	Accuracy (%)	Parameters
*BLSTM (baseline)	45.52	~ 0.9 M
*GCN (baseline)	56.03	~ 92 K
*PATCHY-SAN [35]	48.42	~ 80 K
*PATCHY-Diff [61]	55.29	~ 71 K
Trajectory learning [55]	50.00	-
*L-GrIN	58.59	~ 110 K

* use same node features

Results. Table 3 shows that our model performs better than the baselines and state-of-the-art methods on IEMOCAP. Note that PATCHY-SAN and PATCHY-Diff perform better than BLSTM and CNN-LSTM methods, indicating the effectiveness of graph-based methods in general.

4.3 Body emotion recognition

Databases. We use the MPI emotional body expression database [77] for our experiments. This database contains 1447 body motion samples of actors narrating coherent stories labeled with 11 emotions: *amusement, anger, disgust, fear, joy, neutral, pride, relief, sadness, shame, and surprise*. During their performance, a mocap system (model: Xsens MVN) recorded the human motion using miniature inertial sensors. The system recorded dynamic 3D postures from 22 joints with a sampling rate of 120Hz.

Node features. For this database, we use the raw information provided by the mocap system as input. Each node contains the 3D positions and orientations (measure in terms of the Euler angles) at a given time-step. The feature consists of Euler angles from 22 joints and additional location information of the reference point. We use all this information (without any preprocessing) as node features, resulting into a vector dimension of $P = 72$.

Implementation details. Each input sample produces a graph of $M = 120$ nodes, where each node corresponds to a temporal segment of 120^{th} of a second. Cyclic padding is used as before. We perform a 5-fold cross-validation and report the average accuracy in Table 4. All other network parameters remain the same as before.

Table 5: Comparison between learnable and fixed pooling strategies on the RML database. All experiments use the same binary adjacency matrix for fair comparison.

Pooling strategy	Maxpool	Meanpool	Sortpool [78]	Learnable
Accuracy (%)	89.76	90.23	83.66	91.50

Table 6: Comparison between learnable and manually constructed graph structures. For fair comparison, all experiments use only maxpool to obtain graph embedding.

Adjacency (A)	Binary	Weighted	Learnable
Accuracy (%)	89.54	62.45	91.50

Baselines, state-of-the-art. Our model is compared with the baselines (BLSTM and GCN), the state-of-the-art graph-based architectures (PATCHY-SAN and PATCHY-Diff), and a recent work on this database, i.e., trajectory learning [55]. The trajectory learning system [55] models neural motion and analyzes the spectral difference between an expressive motion and a neutral motion in order to recognize the body expressions.

Results. Table 4 shows that L-GrIN outperforms the baselines and state-of-the-art methods on the MPI body expression database. Graph-based methods continue to perform well, indicating the effectiveness of graph-based methods for such tasks. Fig. 5 shows the learned adjacency A for the MPI database. As before, the learned graph structure exhibit higher temporal dependencies among the neighboring nodes.

4.4 Network analysis

Network size. Tables 1, 3 and 4 list the number of learnable network parameters for the baselines, state-of-the-art graph-based architectures and the proposed L-GrIN. As mentioned earlier, a graph network largely reduces the number of learnable parameters as compared to the BLSTM or CNN architectures such as SENet (see Table 1) without compromising the recognition accuracy. Our model has more parameters than the baseline GCN due to the inception layers and other learnable parameters, but also improves the recognition accuracy significantly. PATCHY-SAN and PATCHY-Diff have smaller network size compared to L-GRIN, but both trail L-GrIN in terms of performance on all databases. In case of facial emotion recognition, we discount the model size of the landmark detector in the comparison as it is common to all except SENet. For speech and body emotion recognition, no additional network was required for as we used hand-crafted features and raw data.

Learnable vs. fixed pooling. Recall that to obtain a graph-level embedding from node-level embeddings, L-GrIN learns a pooling function (see Fig. 2). To show if learnable pooling indeed improves the recognition performance, we compare its performance with various fixed pooling strategies: max pooling, mean pooling

Table 7: Ablation study on the RML database. Each new component in L-GRIN contributes towards its performance.

$\mathcal{G}^* \text{conv}$	Inception	Learned A	Learned p	Accuracy (%)
-	-	-	-	76.57
✓	-	-	-	80.12
-	✓	-	-	87.58
-	-	✓	-	79.78
-	-	-	✓	82.86
-	-	✓	✓	84.21
✓	✓	-	-	90.65
✓	✓	✓	-	91.50
✓	✓	-	✓	91.50
✓	✓	✓	✓	94.11

and sort pooling (sortpool) [78]. Table 5 presents the comparisons on the RML database in terms of facial emotion recognition accuracy, which clearly shows the advantage of learnable pooling over fixed pooling strategies. Similar trend is observed for other databases. Table 6 compares the performance between the proposed learnable adjacency (with max pooling, *not* learnable pooling) idea with the two fixed adjacency matrices on the RML database. Learnable adjacency matrix shows clear advantage in terms of performance. Similar trend is observed for other databases.

Ablation study. We performed exhaustive ablation experiments to investigate the contribution of each component we proposed to build L-GrIN. Table 7 presents the ablation results on the RML database. We observe that each new component brings significant improvement (row 2 to row 5) over the performance of standard GCN [23] which has 76.57% recognition accuracy (the top row in Table 7). The introduction of the graph inception layer increases the recognition rate by 11%; when combined with our new graph convolution layer $\mathcal{G}^* \text{conv}$ (Eq. (4)), the accuracy increases to 90.65%. Adding the learnable graph structure (learned A) and learnable pooling bring the accuracy up to 94.11% both contributing to the accuracy. Removing either of the learnable components reduces the accuracy by 2.61%. The ablation results show that each of the proposed components in our architecture is important, and contributes positively towards its superior performance. Similar ablation trend was observed for other databases.

Qualitative results. To get an insight into the learning process of our model we visualized how it attends to different nodes. Since the video data is the most suitable for this, we used our trained model on RAVDESS. We then feed-forward each test sample through the network, and identify the node (each node corresponds to a video frame) that responded most strongly towards the max-pooling layer. This yields a *salient* node corresponding to each input. We present the corresponding video frames - one example per emotion class for RAVDESS in Fig. 7. The results show that the proposed model is able to learn the salient information from the input graphs such that it is representative of each emotion.



Figure 7: Qualitative results showing the node (frame) for a graph input that generated the strongest response in our network. One result is displayed per class for RAVDESS. This shows that L-GRIN is able to learn the salient information for each emotion.

5 CONCLUSION

We proposed a novel, generalized graph convolution architecture that can recognize emotion in any dynamic input sequence, such as video and speech. Our architecture, L-GrIN, learns to detect emotion while jointly learning the underlying graph structure (adjacency matrix capturing the pairwise temporal relationship between nodes) and a pooling function to yield graph-level representation from node-level embeddings. We proposed a new definition of graph convolution and introduced the idea of inception in graph domain. We showed that each new component in L-GRIN contributes to its performance across three modalities (video, audio and motion capture). We achieved state-of-the-art accuracy on four benchmark databases spanning three different modalities outperforming several competitive baselines and existing methods.

We used modality-specific features or even raw data as node features in this work. However, our approach can be trained end-to-end by combining with modality-specific network for feature extraction. The proposed architecture we developed, although focuses on emotion recognition, is fairly generic. It will be applicable to a variety of classification tasks, such as pose estimation, action recognition and visual speech recognition.

REFERENCES

- [1] Yin Zhang, Min Chen, Nadra Guizani, Di Wu, and Victor CM Leung. Sovcan: Safety-oriented vehicular controller area network. *IEEE Communications Magazine*, 55(8):94–99, 2017.
- [2] Nitish Nag, Vaibhav Pandey, Preston J Putzel, Hari Bhimaraju, Srikanth Krishnan, and Ramesh Jain. Cross-modal health state estimation. In *Proceedings of the 26th ACM international conference on Multimedia*, pages 1993–2002, 2018.
- [3] Runnan Li, Zhiyong Wu, Jia Jia, Jingbei Li, Wei Chen, and Helen Meng. Inferring user emotive state changes in realistic human-computer conversational dialogs. In *Proceedings of the 26th ACM international conference on Multimedia*, pages 136–144, 2018.
- [4] Raviteja Vemulapalli and Aseem Agarwala. A compact embedding for facial expression similarity. In *Conference on Computer Vision and Pattern Recognition (CVPR)*, pages 5683–5692, 2019.
- [5] Xiangyun Zhao, Xiaodan Liang, Luoqi Liu, Teng Li, Yugang Han, Nuno Vasconcelos, and Shuicheng Yan. Peak-piloted deep network for facial expression recognition. In *European Conference on Computer Vision (ECCV)*, pages 425–442. Springer, 2016.
- [6] Jiyoung Lee, Seungryong Kim, Sunok Kim, Jungin Park, and Kwanghoon Sohn. Context-aware emotion recognition networks. In *International Conference on Computer Vision (ICCV)*, pages 2893–2901, 2019.
- [7] Shan Li, Weihong Deng, and JunPing Du. Reliable crowdsourcing and deep locality-preserving learning for expression recognition in the wild. In *Conference on Computer Vision and Pattern Recognition (CVPR)*, pages 2852–2861, 2017.

[8] Adria Ruiz, Joost Van de Weijer, and Xavier Binefa. From emotions to action units with hidden and semi-hidden-task learning. In *International Conference on Computer Vision (ICCV)*, pages 3703–3711, 2015.

[9] Yue Gu, Xinyu Lyu, Weijia Sun, Weitian Li, Shuhong Chen, Xinyu Li, and Ivan Marsic. Mutual correlation attentive factors in dyadic fusion networks for speech emotion recognition. In Laurent Amsaleg, Benoit Huet, Martha A. Larson, Guillaume Gravier, Hayley Hung, Chong-Wah Ngo, and Wei Tsang Ooi, editors, *Proceedings of the 27th ACM International Conference on Multimedia, MM 2019, Nice, France, October 21–25, 2019*, pages 157–166. ACM, 2019.

[10] Samuel Albanie, Arsha Nagrani, Andrea Vedaldi, and Andrew Zisserman. Emotion recognition in speech using cross-modal transfer in the wild. In Susanne Boll, Kyoung Mu Lee, Jiebo Luo, Wenwu Zhu, Hyeran Byun, Chang Wen Chen, Rainer Lienhart, and Tao Mei, editors, *2018 ACM Multimedia Conference on Multimedia Conference, MM 2018, Seoul, Republic of Korea, October 22–26, 2018*, pages 292–301. ACM, 2018.

[11] Kun-Yi Huang, Chung-Hsien Wu, Qian-Bei Hong, Ming-Hsiang Su, and Yi-Hsuan Chen. Speech emotion recognition using deep neural network considering verbal and nonverbal speech sounds. In *ICASSP 2019-2019 IEEE International Conference on Acoustics, Speech and Signal Processing (ICASSP)*, pages 5866–5870. IEEE, 2019.

[12] Jian Huang, Ya Li, Jianhua Tao, Zhen Lian, et al. Speech emotion recognition from variable-length inputs with triplet loss function. In *Interspeech*, pages 3673–3677, 2018.

[13] Ronak Kosti, Jose M Alvarez, Adria Recasens, and Agata Lapedriza. Emotion recognition in context. In *Proceedings of the IEEE Conference on Computer Vision and Pattern Recognition*, pages 1667–1675, 2017.

[14] Son Thai Ly, Guee-Sang Lee, Soo-Hyung Kim, and Hyung-Jeong Yang. Emotion recognition via body gesture: Deep learning model coupled with keyframe selection. In *Proceedings of the 2018 International Conference on Machine Learning and Machine Intelligence*, pages 27–31, 2018.

[15] Nesrine Fourati, Catherine Pelachaud, and Patrice Darmon. Contribution of temporal and multi-level body cues to emotion classification. In *2019 8th International Conference on Affective Computing and Intelligent Interaction (ACII)*, pages 116–122. IEEE, 2019.

[16] Jia-Xin Ma, Hao Tang, Wei-Long Zheng, and Bao-Liang Lu. Emotion recognition using multimodal residual LSTM network. In Laurent Amsaleg, Benoit Huet, Martha A. Larson, Guillaume Gravier, Hayley Hung, Chong-Wah Ngo, and Wei Tsang Ooi, editors, *Proceedings of the 27th ACM International Conference on Multimedia, MM 2019, Nice, France, October 21–25, 2019*, pages 176–183. ACM, 2019.

[17] Panagiotis Tzirakis, George Trigeorgis, Mihalis A Nicolaou, Björn W Schuller, and Stefanos Zafeiriou. End-to-end multimodal emotion recognition using deep neural networks. *IEEE Journal of Selected Topics in Signal Processing*, 11(8):1301–1309, 2017.

[18] Seyedmahdad Mirsamadi, Emad Barsoum, and Cha Zhang. Automatic speech emotion recognition using recurrent neural networks with local attention. In *International Conference on Acoustics, Speech and Signal Processing (ICASSP)*, pages 2227–2231, 2017.

[19] Wenjing Han, Huabin Ruan, Xiaomin Chen, Zhiyang Wang, Haifeng Li, and Björn W Schuller. Towards temporal modelling of categorical speech emotion recognition. In *Interspeech*, pages 932–936, 2018.

[20] Yin Fan, Xiangju Lu, Dian Li, and Yuanliu Liu. Video-based emotion recognition using cnn-rnn and c3d hybrid networks. In *ACM International Conference on Multimodal Interaction*, pages 445–450, 2016.

[21] Sijie Yan, Yuanjun Xiong, and Dahua Lin. Spatial temporal graph convolutional networks for skeleton-based action recognition. In *AAAI Conference on Artificial Intelligence*, pages 7444–7452, 2018.

[22] Justin Gilmer, Samuel S Schoenholz, Patrick F Riley, Oriol Vinyals, and George E Dahl. Neural message passing for quantum chemistry. In *International Conference on Machine Learning (ICML)*, pages 1263–1272, 2017.

[23] Thomas N. Kipf and Max Welling. Semi-supervised classification with graph convolutional networks. In *International Conference on Learning Representations (ICLR)*, 2017.

[24] Keyulu Xu, Weihua Hu, Jure Leskovec, and Stefanie Jegelka. How powerful are graph neural networks? In *International Conference on Learning Representations (ICLR)*, 2019.

[25] Jie Zhou, Ganqu Cui, Zhengyan Zhang, Cheng Yang, Zhiyuan Liu, and Maosong Sun. Graph neural networks: A review of methods and applications. *CoRR*, abs/1812.08434, 2018.

[26] THUNLP, Natural Language Processing Lab at Tsinghua University. Must-read papers on GNN. <https://github.com/thunlp/GNNPapers>. Online; accessed 29 January 2014.

[27] Zhongdao Wang, Liang Zheng, Yali Li, and Shengjin Wang. Linkage based face clustering via graph convolution network. In *Conference on Computer Vision and Pattern Recognition (CVPR)*, pages 1117–1125, 2019.

[28] Charles R Qi, Hao Su, Kaichun Mo, and Leonidas J Guibas. Pointnet: Deep learning on point sets for 3d classification and segmentation. In *Conference on Computer Vision and Pattern Recognition (CVPR)*, pages 652–660, 2017.

[29] Damien Teney, Lingqiao Liu, and Anton van den Hengel. Graph-structured representations for visual question answering. In *Conference on Computer Vision and Pattern Recognition (CVPR)*, pages 3233–3241, 2017.

[30] Oron Ashual and Lior Wolf. Specifying object attributes and relations in interactive scene generation. In *International Conference on Computer Vision (ICCV)*, pages 4561–4569, 2019.

[31] Subarna Tripathi, Anahita Bhiwandiwalla, Alexei Bastidas, and Hanlin Tang. Heuristics for image generation from scene graphs. *International Conference on Learning Representations (ICLR) workshop*, 2019.

[32] Roei Herzig, Elad Levi, Huijuan Xu, Eli Brosh, Amir Globerson, and Trevor Darrell. Classifying collisions with spatio-temporal action graph networks. *ICCV Workshop*, 2019.

[33] Yuzong Lin and Katrin Kirchhoff. Graph-based semisupervised learning for acoustic modeling in automatic speech recognition. *IEEE/ACM Transactions on Audio, Speech, and Language Processing*, 24(11):1946–1956, 2016.

[34] Martin Simonovsky and Nikos Komodakis. Dynamic edge-conditioned filters in convolutional neural networks on graphs. In *Conference on Computer Vision and Pattern Recognition (CVPR)*, pages 3693–3702, 2017.

[35] Mathias Niepert, Mohamed Ahmed, and Konstantin Kutzkov. Learning convolutional neural networks for graphs. In *International Conference on Machine Learning (ICML)*, pages 2014–2023, 2016.

[36] Will Hamilton, Zhitao Ying, and Jure Leskovec. Inductive representation learning on large graphs. In *Advances in Neural Information Processing Systems*, pages 1024–1034, 2017.

[37] Bingbing Xu, Huawei Shen, Qi Cao, Yunqi Qiu, and Xueqi Cheng. Graph wavelet neural network. In *International Conference on Learning Representations (ICLR)*, 2019.

[38] Joan Bruna, Wojciech Zaremba, Arthur Szlam, and Yann Lecun. Spectral networks and locally connected networks on graphs. In *International Conference on Learning Representations (ICLR)*, 2014.

[39] Michaël Defferrard, Xavier Bresson, and Pierre Vandergheynst. Convolutional neural networks on graphs with fast localized spectral filtering. In *Advances in Neural Information Processing Systems*, pages 3844–3852, 2016.

[40] Jie Hu, Li Shen, and Gang Sun. Squeeze-and-excitation networks. In *Conference on Computer Vision and Pattern Recognition (CVPR)*, pages 7132–7141, 2018.

[41] Bowen Pan, Shangfei Wang, and Bin Xia. Occluded facial expression recognition enhanced through privileged information. In *Proceedings of the 27th ACM International Conference on Multimedia*, pages 566–573, 2019.

[42] Pedro D Marrero Fernandez, Fidel A Guerrero Pena, Tsang Ren, and Alexandre Cunha. Feratt: Facial expression recognition with attention net. In *Conference on Computer Vision and Pattern Recognition Workshops (CVPRW)*, 2019.

[43] Macario O Cordel, Shaojing Fan, Zhiqi Shen, and Mohan S Kankanhalli. Emotion-aware human attention prediction. In *Conference on Computer Vision and Pattern Recognition (CVPR)*, pages 4026–4035, 2019.

[44] Shashank Jaiswal and Michel Valstar. Deep learning the dynamic appearance and shape of facial action units. In *Winter Conference on Applications of Computer Vision (WACV)*, pages 1–8, 2016.

[45] Heechul Jung, Sihaeng Lee, Junho Yim, Sunjeong Park, and Jummo Kim. Joint fine-tuning in deep neural networks for facial expression recognition. In *International Conference on Computer Vision (ICCV)*, pages 2983–2991, 2015.

[46] Jingwei Yan, Wenming Zheng, Zhen Cui, Chuangao Tang, Tong Zhang, and Yuan Zong. Multi-cue fusion for emotion recognition in the wild. *Neurocomputing*, 309:27–35, 2018.

[47] Björn Schuller, Stefan Steidl, and Anton Batliner. The interspeech 2009 emotion challenge. In *Tenth Annual Conference of the International Speech Communication Association*, 2009.

[48] Qin Jin, Chengxin Li, Shizhe Chen, and Huimin Wu. Speech emotion recognition with acoustic and lexical features. In *International Conference on Acoustics, Speech and Signal Processing (ICASSP)*, pages 4749–4753. IEEE, 2015.

[49] Michael Neumann and Ngoi Thang Vu. Attentive convolutional neural network based speech emotion recognition: A study on the impact of input features, signal length, and acted speech. In *INTERSPEECH*, 2017.

[50] Zhengwei Huang, Ming Dong, Qirong Mao, and Yongzhao Zhan. Speech emotion recognition using cnn. In *Proceedings of the 22nd ACM international conference on Multimedia*, pages 801–804, 2014.

[51] Siddique Latif, Rajib Rana, Sara Khalifa, Raja Jurdak, and Julien Epps. Direct modelling of speech emotion from raw speech. *Proc. Interspeech 2019*, pages 3920–3924, 2019.

[52] George Trigeorgis, Fabien Ringeval, Raymond Brueckner, Erik Marchi, Mihalis A Nicolaou, Björn Schuller, and Stefanos Zafeiriou. Adieu features? end-to-end speech emotion recognition using a deep convolutional recurrent network. In *2016 IEEE international conference on acoustics, speech and signal processing (ICASSP)*, pages 5200–5204. IEEE, 2016.

[53] Lorenzo Tarantino, Philip N Garner, and Alexandros Lazaridis. Self-attention for speech emotion recognition. *Proc. Interspeech 2019*, pages 2578–2582, 2019.

[54] Sayan Ghosh, Eugene Laksana, Louis-Philippe Morency, and Stefan Scherer. Representation learning for speech emotion recognition. In *Interspeech*, pages 3603–3607, 2016.

[55] Arthur Crenn, Alexandre Meyer, Rizwan Ahmed Khan, Hubert Konik, and Saïda Bouakaz. Toward an efficient body expression recognition based on the synthesis of a neutral movement. In *Proceedings of the 19th ACM International Conference on Multimodal Interaction*, pages 15–22, 2017.

[56] Tammay Randhavane, Aniket Bera, Kyra Kapsakis, Uttaran Bhattacharya, Kurt Gray, and Dinesh Manocha. Identifying emotions from walking using affective and deep features. *CoRR*, abs/1906.11884, 2019.

[57] Uttaran Bhattacharya, Trisha Mittal, Rohan Chandra, Tammay Randhavane, Aniket Bera, and Dinesh Manocha. STEP: spatial temporal graph convolutional networks for emotion perception from gaits. *CoRR*, abs/1910.12906, 2019.

[58] Christian Szegedy, Wei Liu, Yangqing Jia, Pierre Sermanet, Scott Reed, Dragomir Anguelov, Dumitru Erhan, Vincent Vanhoucke, and Andrew Rabinovich. Going deeper with convolutions. In *Conference on Computer Vision and Pattern Recognition (CVPR)*, pages 1–9, 2015.

[59] Y Wang and L Guan. Recognizing human emotional state from audiovisual signals. *IEEE Transactions on Multimedia*, 10(5):936–946, 2008.

[60] Steven R Livingstone and Frank A Russo. The ryerson audio-visual database of emotional speech and song (ravdess): A dynamic, multimodal set of facial and vocal expressions in north american english. *PLoS one*, 13(5):e0196391, 2018.

[61] Zhitao Ying, Jiaxuan You, Christopher Morris, Xiang Ren, Will Hamilton, and Jure Leskovec. Hierarchical graph representation learning with differentiable pooling. In *Advances in Neural Information Processing Systems*, pages 4800–4810, 2018.

[62] Yaxiong Ma, Yixue Hao, Min Chen, Jincai Chen, Ping Lu, and Andrej Košir. Audio-visual emotion fusion (avef): A deep efficient weighted approach. *Information Fusion*, 46:184–192, 2019.

[63] Yongjin Wang, Ling Guan, and Anastasios N Venetsanopoulos. Kernel cross-modal factor analysis for information fusion with application to bimodal emotion recognition. *IEEE Transactions on Multimedia*, 14(3):597–607, 2012.

[64] Kah Phooi Seng, Li-Minn Ang, and Chien Shing Ooi. A combined rule-based & machine learning audio-visual emotion recognition approach. *IEEE Transactions on Affective Computing*, 9(1):3–13, 2016.

[65] Esam Ghaleb, Mirela Popa, and Stylianos Asteriadis. Multimodal and temporal perception of audio-visual cues for emotion recognition. In *International Conference on Affective Computing & Intelligent Interaction (ACII)*, 2019.

[66] Jinwei Gu, Xiaodong Yang, Shalini De Mello, and Jan Kautz. Dynamic facial analysis: From bayesian filtering to recurrent neural networks. In *IEEE Conference on Computer Vision and Pattern Recognition*, pages 1548–1557, 2017.

[67] Adrian Bulat and Georgios Tzimiropoulos. How far are we from solving the 2d & 3d face alignment problem?(and a dataset of 230,000 3d facial landmarks). In *International Conference on Computer Vision (ICCV)*, pages 1021–1030, 2017.

[68] Xavier Glorot and Yoshua Bengio. Understanding the difficulty of training deep feedforward neural networks. In *International Conference on Artificial Intelligence and Statistics*, pages 249–256, 2010.

[69] Alex Graves and Jürgen Schmidhuber. Framewise phoneme classification with bidirectional lstm and other neural network architectures. *Neural Networks*, 18(5-6):602–610, 2005.

[70] Ming Tan, Cicero dos Santos, Bing Xiang, and Bowen Zhou. Lstm-based deep learning models for non-factoid answer selection. *International Conference on Learning Representations (ICLR) workshop*, 2016.

[71] Albert Zeyer, Patrick Doetsch, Paul Voigtlaender, Ralf Schlüter, and Hermann Ney. A comprehensive study of deep bidirectional lstm rnns for acoustic modeling in speech recognition. In *International Conference on Acoustics, Speech and Signal Processing (ICASSP)*, pages 2462–2466, 2017.

[72] Zhengxuan Wu, Xiyu Zhang, Tan Zhi-Xuan, Jamil Zaki, and Desmond Ong. Attending to emotional narratives. In *International Conference on Affective Computing & Intelligent Interaction (ACII)*, 2019.

[73] Olivier Martin, Irene Kotsia, Benoit Macq, and Ioannis Pitas. The enterface’05 audio-visual emotion database. In *International Conference on Data Engineering Workshops (ICDEW)*, pages 8–8, 2006.

[74] Carlos Busso, Murtaza Bulut, Chi-Chun Lee, Abe Kazemzadeh, Emily Mower, Samuel Kim, Jeannette N Chang, Sungbok Lee, and Shrikanth S Narayanan. Iemocap: Interactive emotional dyadic motion capture database. *Language resources and evaluation*, 42(4):335, 2008.

[75] Florian Eyben, Martin Wöllmer, and Björn Schuller. Openearfl! introducing the munich open-source emotion and affect recognition toolkit. In *2009 3rd international conference on affective computing and intelligent interaction and workshops*, pages 1–6. IEEE, 2009.

[76] Karttikeya Mangalam and Tanaya Guha. Learning spontaneity to improve emotion recognition in speech. *Proc. Interspeech 2018*, pages 946–950, 2018.

[77] Ekaterina Volkova, Stephan De La Rosa, Heinrich H Büthhoff, and Betty Mohler. The mpi emotional body expressions database for narrative scenarios. *PLoS one*, 9(12), 2014.

[78] Muhan Zhang, Zhicheng Cui, Marion Neumann, and Yixin Chen. An end-to-end deep learning architecture for graph classification. In *AAAI Conference on Artificial Intelligence*, pages 4438–4445, 2018.